

# Clustering of fuel droplets and quality of spray in diesel engines

Tov Elperin,<sup>1,\*</sup> Nathan Kleeorin,<sup>1,†</sup> Michael A. Liberman,<sup>2,‡</sup>  
Victor S. L'vov,<sup>3,§</sup> Anna Pomyalov,<sup>3,¶</sup> and Igor Rogachevskii<sup>1,\*\*</sup>

<sup>1</sup> The Pearlstone Center for Aeronautical Engineering Studies, Department of Mechanical Engineering,  
Ben-Gurion University of the Negev, P. O. Box 653, Beer-Sheva 84105, Israel

<sup>2</sup> Department of Physics, Uppsala University, Box 530, SE-751 21, Uppsala, Sweden

<sup>3</sup> Department of Chemical Physics, The Weizmann Institute of Science, Rehovot 76100, Israel

(Dated: May 22, 2019)

One of the most important requirements to the fuel spray injected into combustion chamber is a high quality of spray atomization. The main qualitative conclusion of this study is that contrary to the paradigm that turbulence in the combustion chamber improves mixing of liquid fuel and air, it may result also in the fuel droplets clustering and hindering the spray atomization and evaporation. Theory of the droplets clustering is developed and applied to the typical conditions of direct injection engines. The spray quality is evaluated for the conditions pertinent to turbulence in diesel engines.

PACS numbers: 47.27.Qb, 05.40.-a.

## I. INTRODUCTION

Diesel engines are widely used during more than hundred years. After continued improvements and developments, the advanced diesel engines have a thermal efficiency exceeding 50%, unreachable so far for both internal and external combustion engines. Since no other types of engine, able to compete and replace the diesel engines, seem to be available we can expect their further increasing usage in the nearest future.

In diesel engines (see, e.g., Refs. [1–3]), the fuel is injected directly into the combustion chamber at a pressure of 300–1500 atm through a multi-hole nozzle with several orifices of 0.15–0.35 mm in diameter. The spray combustion is widely used providing a practical method for rapid vaporization and mixing of liquid fuels with an air. For combustion applications the mechanisms of spray atomization and mixing are of primary importance. The conversion of the high speed liquid columns injected into air into a multitude of individual fluid drops of 10–100  $\mu\text{m}$  in diameter occurs via a multi-stage process, including the fluid mechanics instabilities (e.g., Rayleigh-Taylor instability), followed by their nonlinear stage, appearance of flat fluid sheets, annular and conical sheets, jets, etc. This phenomenon is called an “*atomization process*”. The recent trend of improving the fuel quality highlights the need for better understanding of the process of spray atomization.

The air in the combustion chamber is preliminary heated up to 1000–1200 K in the process of multiple (up to 15 - 20 times) fast compressions. The suitable design of the inlet port and of the combustion chamber provides a preliminary level of turbulent activity, which is further enhanced by the energy intake from the high speed fuel jet. The aerodynamic turbulence enhances mixing of the small fuel droplets with the air, creating presumably well mixed fuel spray.

The fuel combustion in diesel chambers is strongly affected by parameters of the high pressure spray, see, e.g., Refs. [1, 4]. The criterion of injection quality is demanding since both, the good atomization and dispersion, are required over a wide range of fuel flows. In diesel engines, the poor injector performance can result in excessive emission of pollutants and incomplete combustion. The required degree of atomization depends primarily upon the time available for the vaporization. This time is about a few milliseconds, and thus very small droplets are required. For instance, for a gasoline droplet with a diameter of 80  $\mu\text{m}$ , the vaporization requires tens milliseconds. By contrast, the vaporization of a 25  $\mu\text{m}$  droplet requires only a few milliseconds. Since the air utilization is important, the injector should provide both the penetration and the dispersion of the fuel droplets. Typically, however, the high penetration is achieved only by impairing the dispersion. The diesel spray penetrates well through very a dense air, but has a narrow cone angle and a very dense liquid core. Although various breakup regimes have been identified, modelling of the breakup mechanisms remains difficult. The comprehensive computational studies of the spray have been made by many researchers (for a review see, e.g., [4]), in particular using the KIVA code. Nevertheless, the state of the art computational fluid dynamics codes do not allow to calculate two-phase turbulent flows in diesel engines with the required degree of accuracy, and engineers still depend on the empirical formulation. Therefore an understanding of the basic physical processes that determine the parameters of the fluid atomization (like penetration

---

\*Electronic address: [elperin@menix.bgu.ac.il](mailto:elperin@menix.bgu.ac.il); URL: <http://www.bgu.ac.il/~elperin>

†Electronic address: [nat@menix.bgu.ac.il](mailto:nat@menix.bgu.ac.il)

‡Electronic address: [Michael.Liberman@dec11.fysik.uu.se](mailto:Michael.Liberman@dec11.fysik.uu.se); URL: <http://lili.fysik.uu.se/>

§Electronic address: [Victor.Lvov@Weizmann.ac.il](mailto:Victor.Lvov@Weizmann.ac.il); URL: <http://lvov.weizmann.ac.il>

¶Electronic address: [Anna.Pomyalov@Weizmann.ac.il](mailto:Anna.Pomyalov@Weizmann.ac.il)

\*\*Electronic address: [gary@bgumail.bgu.ac.il](mailto:gary@bgumail.bgu.ac.il); URL: <http://www.bgu.ac.il/~gary>

and dispersion) is of paramount importance for increasing the thermal efficiency of diesel engines and decreasing the level of emitted pollutants.

The goal of this study is to analyze the droplet-air interaction leading to the formation of strong inhomogeneities of droplets distribution, referred to as *droplet clustering* (see, e.g., [5] and references therein). Droplets clustering is a consequence of a spontaneous breakdown of their homogeneous space distribution. As a result of the nonlinear stage of clustering, the local density of droplets may rise by hundreds of times and strongly increase the probability of droplet-droplet collisions that lead to their coalescence. Hence, clustering results in appearance (or increasing the amount) of relatively large fuel droplets in the combustion chamber. The important role of clustering instability in the internal combustion engines was emphasized in Ref. [6].

Clearly, the formation and evolution of droplets inhomogeneities (clusters) are of fundamental significance not only in the combustion engineering, but also in many areas of environmental sciences, physics of the atmosphere and meteorology (e. g. smog and fog formation, rain formation), transport and mixing in industrial turbulent flows (like spray drying, cyclone dust separation, abrasive water-jet cutting), see e.g., [7] and references therein. Indeed, the analysis of the experimental data showed that the spatial distributions of droplets in clouds are strongly inhomogeneous [8]. The small-scale inhomogeneities in particles distribution were observed also in laboratory turbulent flows [9, 10].

It was suggested [6, 11] that the main reason for the particle clustering is their inertia: the particles inside the turbulent eddies are carried out to the boundary regions between the eddies by the inertial forces. This mechanism of the preferential concentration acts in all scales of turbulence, increasing toward small scales. Later, this was contested in [12, 13] using the so-called "Kraichnan model" [14] of turbulent advection by the delta-correlated in time random velocity field, whereby the clustering instability did not occur. However, it was shown in [5] that accounting for a finiteness of correlation time of the fluid velocity field results in the clustering instability of heavy particles. The detailed theory of the clustering instability of the inertial particles advected by a turbulent velocity field was developed in Ref. [5] and applied to the dynamics of water droplets in the turbulent atmosphere, related to the problem of rain triggering.

In the present study we apply and further develop this theory to the dynamics of fuel droplets injected into the combustion chamber of diesel engines. The paper organized as follows. In Sec. II we present a qualitative analysis of the droplets instability that causes formation of clusters in a turbulent flow field. In Sec. III we evaluate the characteristic parameters that affect clusters formation as a result of the clustering instability: the droplet response time  $\tau_{dr}$ , the Kolmogorov micro-scale time  $\tau_\eta$ , the characteristic velocity of small and large fuel droplets in turbulent air; the degree of compressibility of

the droplet velocity field,  $\sigma_v(a)$ , where  $a$  is the droplet size. In Sec. III B we study the velocity of small and large fuel droplets in the turbulent air, required for evaluation of the effect of turbulent diffusion in these two regimes. In Sec. IV we present a quantitative analysis for the clustering instability of the second moment of droplets number density. This allows us to generalize the criterion of the clustering instability, obtained in [5]. Finally, in Sec. V C we overview the nonlinear effects which lead to saturation of the clustering instability and determine the droplets number density in the cluster. The latter parameter eventually affects the spray quality. In Sec. V, we present numerical estimates for the conditions of practical interest for diesel engines. The developed theory highlights the choice for the optimal engine speed corresponding to the optimal spray atomization in engines.

## II. CLUSTERING OF FUEL DROPLETS IN TURBULENT GAS

### A. Basic Equations

To analyze dynamics of fuel droplet we use the standard continuous media approximation, introducing the number density  $n(t, \mathbf{r})$  of fuel droplets. The droplets will be treated as spherical particles with radius  $a$ .

The fuel droplets are advected by a turbulent velocity field  $\mathbf{u}(t, \mathbf{r})$ . Since typically the velocity of the carrier gas is much smaller than the sound velocity, the incompressibility constrain  $\text{div } \mathbf{u}(t, \mathbf{r}) = 0$  is applicable. It will be shown below that the fact that droplet density  $\rho_{dr}$  is much larger than the density  $\rho_{air}$  of the ambient gas (typically,  $\rho_{dr}/\rho_{air} \approx 34$ ) is of crucial importance for the clustering instability. Indeed, for heavy droplets  $\mathbf{v}(t, \mathbf{r}) \neq \mathbf{u}(t, \mathbf{r})$  due to the droplets inertia. Therefore, the compressibility of the droplet velocity field  $\mathbf{v}(t, \mathbf{r})$  must be taken into account, since the growth rate of the clustering instability,  $\gamma$ , is proportional to  $\langle |\text{div } \mathbf{v}(t, \mathbf{r})|^2 \rangle$ , where  $\langle \cdot \rangle$  denotes ensemble average.

Let  $\Theta(t, \mathbf{r})$  be the deviation of the droplet number density  $n(t, \mathbf{r})$  from its uniform mean value  $\bar{n} \equiv \langle n \rangle$ :

$$\Theta(t, \mathbf{r}) = n(t, \mathbf{r}) - \bar{n}. \quad (2.1)$$

The pair correlation function of  $\Theta(t, \mathbf{r})$  is defined as

$$\Phi(\mathbf{R}, \mathbf{r}, t) \equiv \langle \Theta(t, \mathbf{r} + \mathbf{R})\Theta(t, \mathbf{r}) \rangle. \quad (2.2)$$

For the sake of simplicity we will consider only a spatially homogeneous, isotropic case when  $\Phi(\mathbf{R}, \mathbf{r}, t)$  depends only on the separation distance  $R$  and time  $t$ :

$$\Phi(t, \mathbf{R}, \mathbf{r}) \rightarrow \Phi(t, R). \quad (2.3)$$

Denote the probability of the pair collisions between droplets as  $p(t)$  which can be expressed as

$$p(t) \propto c \left\{ 1 + \frac{\langle [n(t, \mathbf{r})]^2 \rangle}{\bar{n}^2} \right\} = c \left[ 1 + \frac{\Phi(t, 0)}{\bar{n}^2} \right]. \quad (2.4)$$

Obviously, a large increase of  $\Phi(t, R)$  above the level of  $\bar{n}^2$  leads to a strong growth in the frequency of the droplet collisions.

In the analytical treatment of the problem we use the standard equation for  $n(t, \mathbf{r})$ :

$$\frac{\partial n(t, \mathbf{r})}{\partial t} + \nabla \cdot [n(t, \mathbf{r})\mathbf{v}(t, \mathbf{r})] = D\Delta n(t, \mathbf{r}), \quad (2.5)$$

where  $D$  is the coefficient of molecular (Brownian) diffusion. The equation for  $\Theta(t, \mathbf{r})$  (Eq. (2.1)), follows from Eq. (2.5):

$$\begin{aligned} \frac{\partial \Theta(t, \mathbf{r})}{\partial t} + [\mathbf{v}(t, \mathbf{r}) \cdot \nabla] \Theta(t, \mathbf{r}) \\ = -\Theta(t, \mathbf{r}) \operatorname{div} \mathbf{v}(t, \mathbf{r}) + D\Delta \Theta(t, \mathbf{r}). \end{aligned} \quad (2.6)$$

Here we neglected the term  $\propto \bar{n} \operatorname{div} \mathbf{v}$ , describing the effect of an external source of fluctuations. It was shown in [5] that this effect is usually much smaller than the effect of self-excitation of fluctuations.

One can use Eq. (2.6) to derive equation for  $\Phi(t, R)$  by averaging the equation for  $\Theta(t, \mathbf{r} + \mathbf{R})\Theta(t, \mathbf{r})$  over statistics of the advected turbulent velocity field  $\mathbf{v}(t, \mathbf{r})$ . In general this procedure is quite involved even for simple models of the advecting velocity fields, see, e.g., [5]. Nevertheless, the qualitative understanding of the underlying physics of the clustering instability, leading to both, the exponential growth of  $\Phi(t, R)$  and its nonlinear saturation, can be elucidated by a more simple and transparent analysis, that is presented below.

## B. Qualitative analysis of the clustering instability

### 1. On Richardson-Kolmogorov cascade theory of turbulence

In our discussion we will use the well known Richardson-Kolmogorov cascade theory of turbulence (see, e.g., [15–17]). For the large Reynolds numbers  $Re \gg 1$  the characteristic scale  $L$  of energy injection (outer scale) is much larger than the length of the dissipation scales (*viscous scale*  $\eta$ )  $L \gg \eta$ . In the so-called *inertial interval* of scales, where  $L > r > \eta$ , the statistics of turbulence within the Kolmogorov theory is governed by the only dimensional parameter,  $\varepsilon$ , the rate of the turbulent energy dissipation. Then, the velocity  $u(r)$  and the energy of turbulent motion  $E(r)$  at the characteristic scale  $r$  (referred below as *r-eddies*) may be found by the dimensional reasoning:

$$u(r) \approx (\varepsilon r)^{1/3}, \quad E(r) = \frac{1}{2} \rho_{\text{air}} [u(r)]^2. \quad (2.7)$$

Similarly, the turnover time of *r-eddies*,  $\tau(r)$ , which is of the order of their life time, may be estimated as

$$\tau(r) \approx r/u(r) \approx \varepsilon^{-1/3} r^{2/3}. \quad (2.8)$$

To elucidate the clustering instability let us consider a cluster of droplets with a characteristic scale  $\ell$  moving

with the velocity  $\mathbf{V}_{\text{cl}}(t)$ . The scale  $\ell$  is a parameter which governs the growth rate of the clustering instability,  $\gamma$ . It sets the bounds for two distinct intervals of scales:  $L > r > \ell$  and  $\ell > r > \eta$ . However, if the size of droplets  $a$  is larger than the viscous scale  $\eta$ , the second range of scales becomes  $\ell > r > a$ , because we cannot consider scales which are smaller than the size of particles. Large *r-eddies* with  $r > \ell$  sweep the  $\ell$ -cluster as a whole and determine the value of  $\mathbf{V}_{\text{cl}}(t)$ . This results in the diffusion of the clusters, and eventually affects their distribution in the combustion chamber. The small *r-eddies* determine the dynamics of droplets inside the cluster. The role of these eddies is multifold. First, they lead to the turbulent diffusion of the droplets within the scale of a cluster size. Second, due to the droplets inertia they tend to accumulate droplets in the regions with small vorticity, which leads to the preferential concentration of the droplets. Third, the droplet inertia also causes a transport of fluctuations of droplets number density from smaller scales to larger scales, i.e., in regions with larger turbulent diffusion. The latter can decrease the growth rate of the clustering instability (see below). Thus, the clustering is determined by the competition between these three processes.

### 2. Effect of turbulent diffusion

We consider Eq. (2.6) for  $\Theta(t, \mathbf{r})$  in the coordinate system co-moving with the  $\ell$ -cluster and assume  $\mathbf{v}(t, \mathbf{r}) \approx \mathbf{u}(t, \mathbf{r})$ . In this reference frame the advected velocity  $\mathbf{v}(t, \mathbf{r})$  should be replaced by  $[\mathbf{v}(t, \mathbf{r}) - \mathbf{V}_{\text{cl}}(t)]$ . In particular, the advection term in Eq. (2.6) takes the form

$$\text{Adv} \equiv \{[\mathbf{v}(t, \mathbf{r}) - \mathbf{V}_{\text{cl}}(t)] \cdot \nabla\} \Theta(t, \mathbf{r}). \quad (2.9)$$

This term leads to the turbulent diffusion of droplets. It is well known (see, e.g. [16]) that the turbulent diffusion can be modelled by the renormalization of the diffusion term in the right hand side (RHS) of Eq. (2.6):

$$D \Rightarrow D + D_{\text{T}}, \quad (2.10)$$

where  $D_{\text{T}}$  is the turbulent diffusion coefficient. The main contribution to the advected velocity in Eq. (2.9) is due to the velocity of  $\ell$ -eddies,  $v(\ell)$ . Therefore  $D_{\text{T}}$  becomes a function of scale  $\ell$ ,  $D_{\text{T}} \Rightarrow D_{\text{T}}(\ell)$ , and can be estimated from the parameters of  $\ell$ -eddies, using dimensional reasoning:

$$D_{\text{T}}(\ell) \approx \frac{1}{3} \ell v(\ell). \quad (2.11)$$

Here we used the commonly accepted [15, 17] numerical factor  $\frac{1}{3}$  for the turbulent diffusion coefficient. Now the part of Eq. (2.6) describing the turbulent diffusion may be written as

$$\frac{\partial \Theta(t, \mathbf{r})}{\partial t} = -D_{\text{T}}(\ell) \Delta \Theta(t, \mathbf{r}). \quad (2.12)$$

During the linear stage of the cluster evolution the droplet distribution inside the cluster does not change. Therefore, the function  $\Theta(t, \mathbf{r})$  in the expression for the correlation function  $\Phi$  in Eq. (2.2) can be factorized:

$$\Theta(t, \mathbf{r}) \Rightarrow A_\ell(t)\theta_\ell(r) . \quad (2.13)$$

Then, Eq. (2.12) yields

$$A_\ell^2(t) = A_\ell^2(0) \exp[-\gamma_{\text{dif}} t], \quad \gamma_{\text{dif}} = \frac{2D_T(\ell)}{\ell^2} \approx \frac{2v(\ell)}{3\ell}, \quad (2.14)$$

where the Laplace operator is evaluated as  $1/\ell^2$  and we used Eq. (2.11).

### 3. Effect of droplets inertia

For the qualitative analysis of the droplets inertia we consider Eq. (2.6), written in the co-moving reference frame, taking into account only inertia term:

$$\frac{\partial \Theta(t, \mathbf{r})}{\partial t} = -\Theta(t, \mathbf{r}) \operatorname{div}[\mathbf{v}(t, \mathbf{r}) - \mathbf{V}_{\text{cl}}(t)] . \quad (2.15)$$

As before we can factorize the function  $\Theta(t, \mathbf{r})$  according to Eq. (2.13) and simplify the partial differential equation (2.15), reducing it to the differential equation for the cluster amplitude  $A_\ell(t)$ :

$$\frac{dA_\ell(t)}{dt} = -A_\ell(t) b_\ell(t) . \quad (2.16)$$

Here we neglected the  $\mathbf{r}$ -dependence of the divergence term inside the cluster in the RHS of Eq. (2.15), so that this term becomes a function of  $t$  only:

$$\operatorname{div}[\mathbf{v}(t, \mathbf{r}) - \mathbf{V}_{\text{cl}}(t)] \Rightarrow b_\ell(t) . \quad (2.17)$$

In the turbulent flow field the function  $b_\ell(t)$  may be considered as a random process with some correlation time  $\tau_b$ , which will be evaluated below. Since the instability of  $\ell$ -clusters is caused by  $\ell$ -eddies, the correlation time  $\tau_b$  can be estimated as the turnover time of the droplet velocity field of  $\ell$ -eddies:

$$\tau_b \approx \ell/v(\ell) . \quad (2.18)$$

The evaluation of the mean square value of  $b_\ell(t)$  requires a more careful consideration. One cannot estimate  $\operatorname{div} \mathbf{v}(\mathbf{r})$  by the dimensional reasoning as  $v(r)/r$ . Indeed, in the incompressible flow  $\operatorname{div} \mathbf{v}(\mathbf{r}) = 0$ . To elucidate this issue we introduce a dimensionless parameter  $\sigma_v$ , a *degree of compressibility* of the velocity field of droplets in  $\ell$ -clusters,  $\mathbf{v}_\ell(t, \mathbf{r})$ , defined by

$$\sigma_v \equiv \langle [\operatorname{div} \mathbf{v}_\ell]^2 \rangle / \langle |\nabla \times \mathbf{v}_\ell|^2 \rangle . \quad (2.19)$$

This parameter may be of the order of 1 (see Refs. [11, 12]); for the turbulence in diesel combustion chambers it will be evaluated in Sec. V below. At the moment we

can evaluate  $b_\ell(t)$  via this yet unknown parameter  $\sigma_v$  as follows:

$$\langle b_\ell(t) \rangle = 0, \quad \langle b_\ell^2(t) \rangle \approx \sigma_v [v(\ell)/\ell]^2 . \quad (2.20)$$

Let us show that the stochastic differential equation (2.16) results in an exponential growth of  $\langle A_\ell^2(t) \rangle$ , i.e. in the instability. Indeed, the solution of this equation reads:

$$A_\ell(t) = A_\ell(0) \exp[-I(t)], \quad I(t) \equiv \int_0^t b_\ell(\tau) d\tau . \quad (2.21)$$

Integral  $I(t)$  may be written as the sum of integrals  $I_n$  over small time intervals  $\tau_b$ :

$$I(t) = \sum_{n=1}^N I_n, \quad I_n \equiv \int_{n\tau_b}^{(n+1)\tau_b} b_\ell(\tau) d\tau, \quad N = \frac{t}{\tau_b} . \quad (2.22)$$

By definition,  $\tau_b$  is the correlation time of the random process  $b_\ell(t)$ . Therefore the integrals  $I_n$  can be considered as independent random variables. According to the central limit theorem, the sum of a large number of statistically independent random variables is distributed as the Gaussian random variable. Therefore the total integral  $I(t)$  can be estimated as

$$I(t) \simeq \sqrt{N \langle I_n^2 \rangle} \tilde{\zeta}, \quad \langle I_n^2 \rangle = \tau_b^2 \langle b_\ell^2(t) \rangle . \quad (2.23)$$

Here  $\tilde{\zeta}$  is a Gaussian random variable with zero mean and unit variance. The probability distribution function of  $\tilde{\zeta}$  reads

$$\mathcal{P}(\tilde{\zeta}) = \frac{1}{\sqrt{2\pi}} \exp\left(-\frac{\tilde{\zeta}^2}{2}\right) . \quad (2.24)$$

Using Eqs. (2.21), (2.24) and (2.22) we obtain

$$\begin{aligned} \langle A_\ell^2(t) \rangle &\simeq A_\ell^2(0) \int \exp[-2\sqrt{N \langle I_n^2 \rangle} \tilde{\zeta}] \mathcal{P}(\tilde{\zeta}) d\tilde{\zeta} \\ &= A_\ell^2(0) \exp[\gamma_{\text{in}} t], \end{aligned} \quad (2.25)$$

where the growth rate  $\gamma_{\text{in}}$  is given by

$$\gamma_{\text{in}} = \frac{N \langle I_n^2 \rangle}{\tau_b} \approx 2\tau_b \langle b_\ell^2(t) \rangle \approx \frac{2\sigma_v v(\ell)}{\ell} . \quad (2.26)$$

In the last estimate we used Eqs. (2.18) and (2.20).

It is clearly seen that the source of the instability is a nonzero value of  $\sigma_v$ , i.e. a *compressibility of the particle (droplet) velocity field*,  $\mathbf{v}(t, \mathbf{r})$ .

In the case of the small enough droplets,  $\tau_{\text{dr}} \leq \tau(\eta)$ , where  $\tau(\eta)$  is the turnover time of the smallest, Kolmogorov micro-scale eddies. In this case all the droplets are almost fully involved in turbulent motion, and one concludes that  $u(t, \mathbf{r}) \approx v(t, \mathbf{r})$  and  $v(\ell) \approx u(\ell)$ . Also we will see below that in this case the largest value of

$\sigma_v$  is attained for  $\ell \approx \eta$ . Hence for  $\tau_{\text{dr}} \leq \tau(\eta)$  the most unstable clusters are those with  $\ell \approx \eta$ . In summary:

- In the case  $\tau_{\text{dr}} \leq \tau(\eta)$ , the characteristic scale of the most unstable clusters of small enough droplets is of the order of Kolmogorov micro-scale of turbulence,  $\eta$ .

- The characteristic growth rate of the clustering instability is of the order of the turnover frequency of  $\eta$ -eddies,  $1/\tau(\eta)$ .

- The droplet clusters are unstable for heavy enough droplets, such that the degree of compressibility  $\sigma_v(\eta)$  of their effective advective velocity field exceeds some threshold value  $\sigma_{\text{cr}} \approx 0.3$  (see [5]).

### III. THE DROPLETS VELOCITY FIELD

In this section we discuss the compressibility of the droplet velocity field. In particular, to clarify the range of validity of the Stokes approximation for the droplet motion in air, in Sec. III A we evaluate the droplet response time  $\tau_{\text{dr}}$  as compared with the Kolmogorov micro-scale time  $\tau_\eta$ . In Sec. III B we study the velocity of small and large fuel droplets in the turbulent air, required for evaluation of the effect of turbulent diffusion in these two regimes. This study also allows us to find the dependence of the degree of compressibility of the droplet velocity field,  $\sigma_v$ , on the droplet response time.

#### A. Characteristic time scales and validity of the Stokes approximation

Let us assume that the radius of the droplets is small, so that the droplet Reynolds number  $\mathcal{R}e_{\text{dr}}$  is smaller than the critical value,  $\mathcal{R}e_{\text{cr}}$ , at which the laminar flow over a droplet loses its stability. Then, we can apply the Stokes approximation. It states that the air-droplet friction force is proportional to the *slip velocity*, the difference between the droplet velocity and the air velocity. A careful analysis performed by Lumley [18] shows that in a turbulent flow the validity condition for  $\mathcal{R}e_{\text{dr}} \leq \mathcal{R}e_{\text{cr}}$  may be expressed via the droplet radius  $a$  and the Kolmogorov micro-scale  $\eta$  as follows:

$$a \leq 2\eta(\rho_{\text{air}}/\rho_{\text{dr}})^{1/3}. \quad (3.1)$$

In the present analysis the ratio of the inertial time scale of the droplets (the Stokes time scale  $\tau_{\text{dr}}$ ) and the turnover time of  $\eta$ -eddies in the Kolmogorov micro-scale  $\tau(\eta)$ , is of primary importance. The droplet response time is given by

$$\tau_{\text{dr}} = \frac{m_{\text{dr}}}{6\pi\nu\rho_{\text{air}}a} = \frac{2\rho_{\text{dr}}a^2}{9\rho_{\text{air}}\nu}, \quad (3.2)$$

where the droplet mass  $m_{\text{dr}}$  is:

$$m_{\text{dr}} = \frac{4\pi}{3}a^3\rho_{\text{dr}}. \quad (3.3)$$

The Kolmogorov micro-scale  $\eta$  is determined from the condition that the Reynolds number for eddies of scale  $\eta$  is equal to 1:

$$\mathcal{R}e_\eta = \eta v(\eta)/\nu = 1. \quad (3.4)$$

Here  $v(\eta)$  is the characteristic velocity of  $\eta$ -scale eddies. It is related to the turnover time of the eddies as  $\tau(\eta) = \eta/v(\eta)$ . This allows us to rewrite the expression (3.4) as follows:

$$\tau(\eta) = \eta^2/\nu. \quad (3.5)$$

Then, the ratio of the time-scales  $\tau_{\text{dr}}$  and  $\tau(\eta)$  follows from Eqs. (3.2) and (3.5):

$$\frac{\tau_{\text{dr}}}{\tau(\eta)} = \frac{2\rho_{\text{dr}}a^2}{9\rho_{\text{air}}\eta^2}. \quad (3.6)$$

Substituting the condition (3.1) for the validity of the Stokes approximation we find

$$\frac{\tau_{\text{dr}}}{\tau(\eta)} \leq \left(\frac{\rho_{\text{dr}}}{\rho_{\text{air}}}\right)^{1/3}, \quad (3.7)$$

Equation (3.7) implies that for "heavy" droplets in a gas, that satisfy the Stokes approximation, the droplet response time scale may be about ten times larger than the Kolmogorov time scale:  $\tau_{\text{dr}} \leq 10\tau(\eta)$ .

#### B. Droplet velocity in turbulent air

##### 1. Equation for a droplet velocity

Assuming that the droplets are small enough such that Eq. (3.1) is valid, we can apply Stokes' law for the air-droplet friction force  $\mathbf{F}_{\text{dr}}(t, \mathbf{r})$ :

$$\mathbf{F}_{\text{dr}}(t, \mathbf{r}) = \zeta[\mathbf{v}_{\text{dr}}(t, \mathbf{r}) - \mathbf{u}(t, \mathbf{r})], \quad (3.8)$$

with the Stokes friction coefficient  $\zeta$  given by

$$\zeta = 6\pi\rho_{\text{air}}\nu a. \quad (3.9)$$

The Newton equation for a droplet reads:

$$m_{\text{dr}} \frac{d\mathbf{v}_{\text{dr}}(t, \mathbf{r})}{dt} = -\mathbf{F}_{\text{dr}}(t, \mathbf{r}) = \zeta[\mathbf{u}(t, \mathbf{r}) - \mathbf{v}_{\text{dr}}(t, \mathbf{r})]. \quad (3.10)$$

Here the total time derivative ( $d/dt$ ) takes into account the time dependence of the droplet coordinate  $\mathbf{r}$ :

$$\frac{d}{dt} = \left[ \frac{\partial}{\partial t} + \mathbf{v}_{\text{dr}}(t, \mathbf{r}) \cdot \nabla \right]. \quad (3.11)$$

Now Eq. (3.10) takes the form:

$$\left\{ \tau_{\text{dr}} \left[ \frac{\partial}{\partial t} + \mathbf{v}_{\text{dr}}(t, \mathbf{r}) \cdot \nabla \right] + 1 \right\} \mathbf{v}_{\text{dr}}(t, \mathbf{r}) = \mathbf{u}(t, \mathbf{r}). \quad (3.12)$$

In the following we analyze this equation in two limiting cases: for small droplets with  $\tau_{\text{dr}}$  smaller than the turnover time of  $\ell$ -eddies (Sec. III B 2), and for large droplets, in Sec. III B 3.

## 2. Velocity of small droplets

In this section we consider small droplets for which the Stokes time  $\tau_{\text{dr}}$  is smaller than the turnover time of  $\ell$ -eddies,  $\tau(\ell) \approx \ell/u(\ell)$ . These droplets are completely involved in the motion of  $\ell$ -eddies and for  $\tau_{\text{dr}}/\tau(\ell) = 0$ , we can write  $\mathbf{v}_\ell(t, \mathbf{r}) = \mathbf{u}_\ell(t, \mathbf{r})$ . Here subscript " $\ell$ " denotes that we are dealing with the velocity field of  $\ell$ -eddies,  $\mathbf{u}_\ell(t, \mathbf{r})$ , and the velocity of droplets in  $\ell$ -clusters,  $\mathbf{v}_\ell(t, \mathbf{r})$ , that was generated by  $\ell$ -eddies. In this approximation the velocity field  $\mathbf{v}_\ell(t, \mathbf{r})$  is incompressible. Therefore, the compressibility parameter  $\sigma_v$  may be determined by the first order corrections.

To find the corrections to  $\mathbf{v}_\ell(t, \mathbf{r})$  linear in  $\tau_{\text{dr}}$ , we consider a formal solution of Eq. (3.12) in the form:

$$\mathbf{v}_\ell(t, \mathbf{r}) = \left[ \tau_{\text{dr}} \frac{d}{dt} + 1 \right]^{-1} \mathbf{u}_\ell(t, \mathbf{r}) . \quad (3.13)$$

Here the inverse operator is understood as its Taylor series expansion:

$$\mathbf{v}_\ell(t, \mathbf{r}) = \mathbf{u}_\ell(t, \mathbf{r}) - \tau_{\text{dr}} \frac{d\mathbf{u}_\ell(t, \mathbf{r})}{dt} + \frac{\tau_{\text{dr}}^2}{2} \left[ \frac{d\mathbf{u}_\ell(t, \mathbf{r})}{dt} \right]^2 + \dots, \quad (3.14)$$

In the linear in  $\tau_{\text{dr}}$  approximation, this solution becomes

$$\mathbf{v}_\ell(t, \mathbf{r}) = \mathbf{u}_\ell(t, \mathbf{r}) - \tau_{\text{dr}} \left[ \frac{\partial}{\partial t} + \mathbf{u}_\ell(t, \mathbf{r}) \cdot \nabla \right] \mathbf{u}_\ell(t, \mathbf{r}), \quad (3.15)$$

where in the RHS we replaced  $\mathbf{v}_\ell(t, \mathbf{r}) \rightarrow \mathbf{u}_\ell(t, \mathbf{r})$ . Consequently, in this approximation

$$\text{div } \mathbf{u}_\ell(t, \mathbf{r}) = \frac{du_\ell^\alpha(t, \mathbf{r})}{dr^\alpha} \approx \tau_{\text{dr}} \frac{du_\ell^\beta(t, \mathbf{r})}{dr^\alpha} \frac{du_\ell^\alpha(t, \mathbf{r})}{dr^\beta} \quad (3.16)$$

(see [6]). Equation (3.16) allows to determine the compressibility parameter  $\sigma_v$ , (2.19), as follows:

$$\sigma_v \approx \left[ \frac{\tau_{\text{dr}}}{\tau(\ell)} \right]^2 \approx \left( \frac{2\rho_{\text{dr}}}{9\rho_{\text{air}}} \right)^2 \left( \frac{a}{\eta} \right)^4 \left( \frac{\eta}{\ell} \right)^{4/3}. \quad (3.17)$$

In deriving this equation we estimated  $[du_\ell^\alpha(t, \mathbf{r})/dr^\alpha]$  as  $[1/\tau(\ell)]$  and used Eqs. (3.6) and (2.8).

Let  $a_*$  be the characteristic size of droplets for which  $\tau_{\text{dr}} = \tau(\eta)$  for  $\ell = \eta$  and, respectively,  $\sigma_v = 1$ :

$$a_* \equiv \eta \sqrt{9\rho_{\text{air}}/2\rho_{\text{dr}}}. \quad (3.18)$$

Using this notation Eq. (3.17) can be rewritten as

$$\frac{\tau(\ell)}{\tau_{\text{dr}}} \approx \left( \frac{a_*}{a} \right)^2 \left( \frac{\ell}{\eta} \right)^{2/3}, \quad (3.19)$$

$$\sigma_v \approx \left( \frac{a}{a_*} \right)^4 \left( \frac{\eta}{\ell} \right)^{4/3}. \quad (3.20)$$

Equations (3.17) and (3.20) are valid only if  $\sigma_v < 1$ , otherwise the approximation of small  $\tau_{\text{dr}}/\tau(\ell)$  ratio is violated.

## 3. Velocity of large droplets

*a. Effective equation of motion.* In this section we consider the opposite case: the large droplets with  $\tau_{\text{dr}}$  is larger than the turnover time of the smallest eddies in the Kolmogorov microscale  $\tau(\eta)$ , but smaller than the turnover time of the largest eddies  $\tau(L)$ . Denote by  $\ell_*$  the characteristic scale of eddies for which

$$\tau_{\text{dr}} = \tau(\ell_*). \quad (3.21)$$

This scale as well as the particles cluster size was introduced in [6]. The eddies with  $\ell \gg \ell_*$  almost fully involve droplets in their motions, while the eddies with  $\ell \ll \ell_*$  do not affect the droplet motions within the zero order approximation in the ratio  $[\tau(\ell)/\tau_{\text{dr}}] \ll 1$ .

To determine  $\mathbf{v}_\ell(t, \mathbf{r})$  we consider Eq. (3.12) in the co-moving with  $\ell$ -eddies reference system, where the surrounding fluid velocity  $\mathbf{u}$  equals to the relative velocity of the  $\ell$ -eddy at  $\mathbf{r}$ , i.e.,  $\mathbf{u}(t, \mathbf{r}) \Rightarrow \mathbf{u}_\ell(t, \mathbf{r})$ . At this point one has to take into account that the  $\ell$ -eddy is swept out by all  $\ell'$ -eddies of larger scales,  $\ell' > \ell$ , while the droplet participates in motions of  $\ell'$ -eddies with  $\ell' > \ell_* > \ell$ . Therefore, the relative velocity  $U_\ell$  of the  $\ell$ -eddy and the droplet is determined by  $\ell'$ -eddies with the intermediate scales,  $\ell_* > \ell' > \ell$ . This velocity is determined by the contribution of  $\ell_*$ -eddies, and can be considered as a time and space independent constant  $\mathbf{u}_*$  during the life time of the  $\ell$  eddy and inside it. Velocity  $\mathbf{u}_*$  in our approach is random and we have to average the final result over statistics of  $\ell_*$ -eddies. Then Eq. (3.12) becomes

$$\left( \tau_{\text{dr}} \frac{\partial}{\partial t} + 1 \right) \mathbf{v}_\ell(t, \mathbf{r}) = \mathbf{u}_\ell(t, \mathbf{r} + \mathbf{u}_* t) - \tau_{\text{dr}} [\mathbf{v}_\ell(t, \mathbf{r}) \cdot \nabla] \mathbf{v}_\ell(t, \mathbf{r}). \quad (3.22)$$

In Eq. (3.22) the velocity  $\mathbf{u}_\ell$  is calculated at point  $\mathbf{r}$  and the velocity  $\mathbf{v}_\ell$  is at  $\mathbf{r} - \mathbf{u}_* t$ . For the sake of convenience we redefine here  $\mathbf{r} - \mathbf{u}_* t \equiv \mathbf{r}' \Rightarrow \mathbf{r}$  and, respectively,  $\mathbf{r} = \mathbf{r}' + \mathbf{u}_* t \Rightarrow \mathbf{r} + \mathbf{u}_* t$ .

*b. First non-vanishing contribution to  $v_\ell$ .* Clearly,  $v_\ell(t, \mathbf{r}) \ll u_\ell$  for  $\ell \ll \ell_*$ . Therefore we can find the first non-vanishing contribution to  $\mathbf{v}_\ell(t, \mathbf{r})$  in the limit  $[\tau(\ell) \ll \tau_{\text{dr}}]$  by considering the linear version of Eq. (3.22):

$$\left( \tau_{\text{dr}} \frac{\partial}{\partial t} + 1 \right) \mathbf{v}_\ell(t, \mathbf{r}) = \mathbf{u}_\ell(t, \mathbf{r} + \mathbf{u}_* t). \quad (3.23)$$

In the  $\omega, \mathbf{k}$  representation this equation takes the form:

$$(i\omega \tau_{\text{dr}} + 1) \mathbf{v}_\ell(\omega, \mathbf{k}) = \mathbf{u}_\ell(\omega - \mathbf{k} \cdot \mathbf{u}_*, \mathbf{k}), \quad (3.24)$$

that allows one to find the relationship between the second order correlation functions  $F_{v,\ell}^{\alpha\beta}(\omega, \mathbf{k})$  and  $F_{u,\ell}^{\alpha\beta}(\omega, \mathbf{k})$  of the velocity fields  $\mathbf{v}_\ell$  and  $\mathbf{u}_\ell$ :

$$F_{v,\ell}^{\alpha\beta}(\omega, \mathbf{k}) = \frac{1}{\omega^2 \tau_{\text{dr}}^2 + 1} F_{u,\ell}^{\alpha\beta}(\omega - \mathbf{k} \cdot \mathbf{u}_*, \mathbf{k}). \quad (3.25)$$

Functions  $F_{u,\ell}^{\alpha\beta}(\omega, \mathbf{k})$  and  $F_{v,\ell}^{\alpha\beta}(\omega, \mathbf{k})$  are defined as usual:

$$(2\pi)^4 \delta(\omega + \omega') \delta(\mathbf{k} + \mathbf{k}') F_{u,\ell}^{\alpha\beta}(\omega, \mathbf{k}) \quad (3.26)$$

$$\equiv \left\langle v_\ell^\alpha(\omega, \mathbf{k}) v_\ell^\beta(\omega', \mathbf{k}') \right\rangle, \quad \text{etc.}$$

The simultaneous correlation functions are related to their  $\omega$ -dependent counterparts via the integral  $\int d\omega/2\pi$ , e.g.,

$$F_{v,\ell}^{\alpha\beta}(\mathbf{k}) = \int \frac{d\omega}{2\pi} F_{v,\ell}^{\alpha\beta}(\omega, \mathbf{k}). \quad (3.27)$$

The tensorial structure of  $F_{u,\ell}^{\alpha\beta}(\mathbf{k})$  follows from the incompressibility condition and the assumption of isotropy:

$$F_{u,\ell}^{\alpha\beta}(\mathbf{k}) = P^{\alpha\beta}(\mathbf{k}) F_{u,\ell}(k), \quad (3.28)$$

where  $P^{\alpha\beta}(\mathbf{k})$  is the transversal projector:

$$P^{\alpha\beta}(\mathbf{k}) = \delta_{\alpha\beta} - k^\alpha k^\beta / k^2. \quad (3.29)$$

In the inertial range of scales the function  $F_{u,\ell}^{\alpha\beta}(\omega, \mathbf{k})$  may be written in the following form:

$$F_{u,\ell}^{\alpha\beta}(\omega, \mathbf{k}) = P^{\alpha\beta}(\mathbf{k}) F_{u,\ell}(k) \tau(\ell) f[\omega \tau(\ell)]. \quad (3.30)$$

Here the dimensionless function  $f(x)$  is normalized as follows:

$$\int_{-\infty}^{\infty} f(x) dx = 2\pi. \quad (3.31)$$

Now we can average the result (3.25, 3.31) over the statistics of  $\ell_*$ -eddies. Denoting the mean value of some function  $g(x)$  as  $\overline{g(x)}$  we have:

$$\overline{f[(\omega - \mathbf{k} \cdot \mathbf{u}_*) \tau(\ell)]} \approx \overline{\delta[(\omega - \mathbf{k} \cdot \mathbf{u}_*) \tau(\ell)]} \quad (3.32)$$

$$\approx \frac{\ell}{\tau(\ell) u_*} f_* \left( \frac{u_* \omega}{\ell} \right).$$

Here the dimensionless function  $f_*(x)$  has one maximum at  $x = 0$ , and it is normalized according to Eq. (3.31). The particular form of  $f_*(x)$  depends on the statistics of  $\ell_*$ -eddies and our qualitative analysis is not sensitive to this form. Thus, we may choose, for instance:

$$f_*(x) = 2/[x^2 + 1]. \quad (3.33)$$

In Eqs. (3.32) we took into account that the characteristic Doppler frequency of  $\ell$ -eddies (in the random velocity field  $u_*$  of  $\ell_*$ -eddies) may be evaluated as:

$$\gamma_D(\ell) \equiv \sqrt{(\mathbf{k} \cdot \mathbf{u}_*)^2} \simeq u_*/\ell. \quad (3.34)$$

This frequency is much larger than the characteristic frequency width of the function  $f[\omega\tau(\ell)]$  [equal to  $1/\tau(\ell)$ ], and therefore the function  $f(x)$  in Eq. (3.32) may be approximated by the delta function  $\delta(x)$ .

After averaging, Eq. (3.25) may be written as

$$F_{v,\ell}^{\alpha\beta}(\omega, \mathbf{k}) = \frac{P^{\alpha\beta}(\mathbf{k}) f_*(0)}{\omega^2 \tau_{\text{dr}}^2 + 1} \frac{\ell}{u_*} F_{u,\ell}(k). \quad (3.35)$$

Here we took into account that  $\tau_{\text{dr}} \gg \ell/u_*$  that allows us to neglect the frequency dependence of  $f_*(u_* \omega/\ell)$  and to calculate this function at  $\omega = 0$ . Together with Eq. (3.35) this yields

$$F_{v,\ell}^{\alpha\beta}(\mathbf{k}) = P^{\alpha\beta}(\mathbf{k}) F_{u,\ell}(k) \frac{\ell}{\tau_{\text{dr}} u_*}, \quad (3.36)$$

where we used the estimate  $f_*(0) \approx 2$ , that follows from Eq. (3.33).

The equation (3.36) provides the relationship between the mean square relative velocity of  $\ell$ -separated droplets,  $v_\ell$ , and the velocity of  $\ell$ -eddies,  $u_\ell$ :

$$v_\ell \simeq u_\ell \sqrt{\frac{\ell}{\tau_{\text{dr}} u_*}} \simeq u_\ell \sqrt{\frac{\ell}{\ell_*}}. \quad (3.37)$$

*c. Effective non-linear equation.* For a qualitative analysis of the role of the nonlinearity of the droplet behavior in an  $\ell$ -cluster we evaluate  $\nabla$  in the nonlinear term, Eq. (3.22), as  $1/\ell$ , neglecting the spatial dependence and the vector structure. The resulting equation in  $\omega$ -representation reads:

$$(i\omega + \gamma_{\text{dr}}) V_\ell(\omega) = \gamma_{\text{dr}} U_\ell(\omega) + \mathcal{N}_\omega, \quad \gamma_{\text{dr}} = 1/\tau_{\text{dr}},$$

$$\mathcal{N}_\omega = -\frac{1}{2\pi\ell} \int d\omega_1 d\omega_2 \delta(\omega + \omega_1 + \omega_2) V_\ell(\omega_1) V_\ell(\omega_2),$$

$$V_\ell(\omega) = \int v_\ell(t) \exp[-i\omega t] dt, \quad (3.38)$$

$$v_\ell(t) = \frac{1}{2\pi} \int V_\ell(\omega) \exp[i\omega t] d\omega.$$

In the zeroth order (linear) approximation ( $\mathcal{N}_\omega \rightarrow 0$ )

$$V_\ell^{(0)}(\omega) = \frac{\gamma_{\text{dr}} U_\ell(\omega)}{i\omega + \gamma_{\text{dr}}}, \quad (3.39)$$

which is the simplified version of Eq. (3.24). This allows us to find in the linear approximation

$$\langle v_\ell^2(t) \rangle = \int \frac{d\omega}{2\pi} \mathcal{F}_\ell(\omega) = \int \frac{d\omega}{2\pi} \frac{\gamma_{\text{dr}}^2 \overline{F_{u,\ell}(\omega)}}{\omega^2 + \gamma_{\text{dr}}^2}, \quad (3.40)$$

where  $F_{u,\ell}(\omega)$  is the correlation functions of  $U_\ell(\omega)$ :

$$2\pi\delta(\omega + \omega') F_{u,\ell}(\omega) = \langle U_\ell(\omega) U_\ell(\omega') \rangle, \quad (3.41)$$

similarly to Eq. (3.26).

In the limit  $\tau_{\text{dr}} \gg \ell/u_*$  one can neglect in Eq. (3.40) the  $\omega$ -dependence of  $\overline{F_{u,\ell}(\omega)}$ , which has characteristic width  $\ell/u_*$  and conclude:

$$v_{\ell,0}^2 \equiv \langle v_\ell^2(t) \rangle \approx \frac{\gamma_{\text{dr}}}{2} \overline{F_{u,\ell}(0)} \approx u_\ell^2 \frac{\ell \gamma_{\text{dr}}}{u_*} \approx u_\ell^2 \frac{\ell}{\ell_*},$$

$$u_\ell^2 \equiv \langle u_\ell^2(t) \rangle, \quad (3.42)$$

in agreement with Eq. (3.37).

*d. First nonlinear correction.* To evaluate the first nonlinear correction to Eq. (3.42) one has to substitute  $V_\ell(\omega)$  from Eq. (3.39) into Eq. (3.38) for  $\mathcal{N}_\omega$ :

$$V_{\ell,1}(\omega) = -\frac{\gamma_{\text{dr}}^2}{2\pi\ell} \int d\omega_1 d\omega_2 \delta(\omega + \omega_1 + \omega_2) \times \frac{U_\ell(\omega_1)}{i\omega_1 + \gamma_{\text{dr}}} \frac{U_\ell(\omega_2)}{i\omega_2 + \gamma_{\text{dr}}}. \quad (3.43)$$

Using Eq. (3.43) instead of Eq. (3.39) we obtain instead of Eq. (3.40)

$$v_{\ell,1}^2 \equiv \langle [v_{\ell,1}(t)]^2 \rangle = \int \frac{d\omega}{2\pi} F_{u,\ell,1}(\omega), \quad (3.44)$$

$$F_{u,\ell,1}(\omega) = \frac{2\gamma_{\text{dr}}^4}{(\omega^2 + \gamma_{\text{dr}}^2)\ell^2} \int \frac{d\omega_1 d\omega_2}{2\pi} \times \frac{\overline{F_{u,\ell}(\omega_1) F_{u,\ell}(\omega_2)} \delta(\omega + \omega_1 + \omega_2)}{(\omega_1^2 + \gamma_{\text{dr}}^2)(\omega_2^2 + \gamma_{\text{dr}}^2)}.$$

In this derivation we assumed for simplicity the Gaussian statistics of the velocity field.

Now let us estimate

$$v_{\ell,1}^2 \approx \frac{[\overline{F_{u,\ell}(0)}]^2}{\ell^2} \approx \frac{u_\ell^4}{u_*^2} \approx u_\ell^2 \left(\frac{\ell}{\ell_*}\right)^{2/3}, \quad (3.45)$$

that is much larger than the result (3.42) for  $v_{\ell,0}^2$  obtained in the linear approximation. This means that the simple iteration procedure we used is inconsistent, since it involves expansion in large parameter  $[(\ell_*/\ell)^{1/3}]$ .

*e. Renormalized perturbative expansion.* A similar situation with a perturbative expansion occurs in the theory of hydrodynamic turbulence, where a simple iteration of the nonlinear term with respect to the linear (viscous) term, yields the power series expansion in  $\mathcal{R}e^2 \gg 1$ . A way out, used in the theory of hydrodynamic turbulence is the Dyson-Wyld re-summation of one-eddy irreducible diagrams (for details see, e.g., Refs. [19, 20]). This procedure corresponds to accounting for the non-linear (so-called "turbulent" viscosity) instead of the linear, kinematic viscosity. A similar approach in our problem implies that we have to account for the self-consistent, non-linear renormalization of the droplet frequency  $\gamma_{\text{dr}} \Rightarrow \Gamma_{\text{dr}}(\ell)$  in Eq. (3.38) and to subtract the corresponding terms from  $\tilde{\mathcal{N}}_\omega$ . With these corrections, Eq. (3.38) reads:

$$[i\omega + \Gamma_{\text{dr}}(\ell)]V_\ell(\omega) = \gamma_{\text{dr}}U_\ell(\omega) + \tilde{\mathcal{N}}_\omega. \quad (3.46)$$

Here  $\tilde{\mathcal{N}}_\omega$  is the non-linear term  $\mathcal{N}_\omega$  after subtraction of the nonlinear contribution to the difference

$$\Delta_{\text{dr}} \equiv \Gamma_{\text{dr}}(\ell) - \gamma_{\text{dr}} \approx \frac{v_\ell^2/\ell^2}{\Gamma_{\text{dr}}(\ell)}. \quad (3.47)$$

The latter relation actually follows from more a detailed perturbation diagrammatic approach. In our context it

is sufficient to realize that in the limit  $\Gamma_{\text{dr}}(\ell) \gg \gamma_{\text{dr}}$  one may evaluate  $\Gamma_{\text{dr}}(\ell)$  by a simple dimensional reasoning:

$$\Gamma_{\text{dr}}(\ell) \approx v_\ell/\ell, \quad (3.48)$$

which is consistent with Eq. (3.47). In addition, Eq. (3.47) has a natural limiting case  $\Gamma_{\text{dr}}(\ell) \rightarrow \gamma_{\text{dr}}$  when  $v_\ell/\ell \ll \gamma_{\text{dr}}$ . Now using Eq. (3.46) instead of Eq. (3.39) we arrive at:

$$V_\ell^{(0)}(\omega) = \frac{\gamma_{\text{dr}}U_\ell(\omega)}{i\omega + \Gamma_{\text{dr}}(\ell)}. \quad (3.49)$$

Accordingly, instead of the estimates (3.42) one has:

$$\tilde{v}_{\ell,0}^2 \approx u_\ell^2 \frac{\gamma_{\text{dr}}^2 \ell}{\Gamma_{\text{dr}}(\ell) u_*} \approx u_\ell^2 \frac{\gamma_{\text{dr}}}{\Gamma_{\text{dr}}(\ell)} \left(\frac{\ell}{\ell_*}\right). \quad (3.50)$$

The latter equation together with Eq. (3.48) allows to evaluate  $\Gamma_{\text{dr}}(\ell)$  as follows:

$$\Gamma_{\text{dr}}(\ell) \approx \left(\frac{\gamma_{\text{dr}}^2 u_\ell^2}{\ell u_*}\right)^{1/3} \approx \gamma_{\text{dr}} \left(\frac{\ell_*}{\ell}\right)^{1/9}. \quad (3.51)$$

Hence the estimate (3.50) becomes

$$\tilde{v}_{\ell,0}^2 \approx u_\ell^2 \left(\frac{\ell}{\ell_*}\right)^{10/9} \approx u_\ell^2 \left[\frac{\tau(\ell)}{\tau_{\text{dr}}}\right]^{5/3}. \quad (3.52)$$

Repeating the evaluation of the nonlinear correction  $\tilde{v}_{\ell,2}^2$  with the renormalized Eq. (3.46) we find that

$$\tilde{v}_{\ell,1}^2 \approx \tilde{v}_{\ell,0}^2. \quad (3.53)$$

This means that now the expansion parameter is of the order of 1, in accordance with the renormalized perturbation approach.

#### IV. THE CLUSTERING INSTABILITY OF THE SECOND MOMENT OF DROPLETS NUMBER DENSITY

In this section we will present a quantitative analysis for the clustering instability of the second moment of droplets number density.

##### A. Basic equations

To determine the growth rate of the clustering instability let us consider the equation for the two-point correlation function  $\Phi(t, \mathbf{R})$  of droplets number density:

$$\frac{\partial \Phi}{\partial t} = [B(\mathbf{R}) + 2\mathbf{U}(\mathbf{R}) \cdot \nabla + \hat{D}_{\alpha\beta}(\mathbf{R}) \nabla_\alpha \nabla_\beta] \Phi(t, \mathbf{R}), \quad (4.1)$$

(see [5]). The meaning of the coefficients  $B(\mathbf{R})$ ,  $\mathbf{U}(\mathbf{R})$  and  $\hat{D}_{\alpha\beta}(\mathbf{R})$  is as follows:

The function  $B(\mathbf{R})$  is determined by the compressibility of the velocity field and it causes the generation of fluctuations of the number density of droplets.

The vector  $\mathbf{U}(\mathbf{R})$  determines a scale-dependent drift velocity which describes a transport of fluctuations of droplets number density from smaller scales to larger scales, i.e., in the regions with larger turbulent diffusion. The latter can decrease the growth rate of the clustering instability. Note that  $\mathbf{U}(\mathbf{R} = 0) = 0$  whereas  $B(\mathbf{R} = 0) \neq 0$ . For incompressible velocity field  $\mathbf{U}(\mathbf{R}) = 0$ ,  $B(\mathbf{R}) = 0$ .

The scale-dependent tensor of turbulent diffusion  $\hat{D}_{\alpha\beta}(\mathbf{R})$  is also affected by the compressibility. In very small scales this tensor is equal to the tensor of the molecular (Brownian) diffusion, while in the vicinity of the maximum scale of turbulent motions this tensor coincides with the regular tensor of turbulent diffusion.

Thus, the clustering instability is determined by the competition between these three processes. The tensor  $\hat{D}_{\alpha\beta}(\mathbf{R})$  may be written as

$$\begin{aligned}\hat{D}_{\alpha\beta}(\mathbf{R}) &= 2D\delta_{\alpha\beta} + D_{\alpha\beta}^{\text{T}}(\mathbf{R}), \\ D_{\alpha\beta}^{\text{T}}(\mathbf{R}) &= \tilde{D}_{\alpha\beta}^{\text{T}}(0) - \tilde{D}_{\alpha\beta}^{\text{T}}(\mathbf{R}).\end{aligned}\quad (4.2)$$

The form of the coefficients  $B(\mathbf{R})$ ,  $\mathbf{U}(\mathbf{R})$  and  $\hat{D}_{\alpha\beta}(\mathbf{R})$  depends on the model of turbulent velocity field. For instance, for the random velocity with Gaussian statistics of the Lagrangian trajectories  $\boldsymbol{\xi}(\mathbf{r}|t)$  these coefficients are given by

$$\begin{aligned}B(\mathbf{R}) &\approx 2 \int_0^\infty \langle b[0, \boldsymbol{\xi}(\mathbf{r}_1|0)] b[\tau, \boldsymbol{\xi}(\mathbf{r}_2|\tau)] \rangle d\tau, \\ \mathbf{U}(\mathbf{R}) &\approx -2 \int_0^\infty \langle \mathbf{v}[0, \boldsymbol{\xi}(\mathbf{r}_1|0)] b[\tau, \boldsymbol{\xi}(\mathbf{r}_2|\tau)] \rangle d\tau, \\ \tilde{D}_{\alpha\beta}^{\text{T}}(\mathbf{R}) &\approx 2 \int_0^\infty \langle v_\alpha[0, \boldsymbol{\xi}(\mathbf{r}_1|0)] v_\beta[\tau, \boldsymbol{\xi}(\mathbf{r}_2|\tau)] \rangle d\tau\end{aligned}\quad (4.3)$$

(for details see [5]), where  $b = \text{div } \mathbf{v}$ .

## B. Clustering instability

Let us study the clustering instability. Consider the range of scales  $a \leq \ell \ll \ell_*$ , where the size of a droplet  $a \geq \eta$ . Then the relationship between  $\tilde{v}_{\ell,0}^2$  and  $u_\ell^2$  reads:

$$\tilde{v}_{\ell,0}^2 = u_\ell^2 \left[ \frac{\tau(\ell)}{\tau_{\text{dr}}} \right]^s, \quad (4.4)$$

where according to Eq. (3.52) the exponent  $s = 5/3$ . In this case the expression for the turbulent diffusion tensor in nondimensional form reads

$$\begin{aligned}D_{\alpha\beta}^{\text{T}}(\mathbf{R}) &= R^{(4s-7)/3} (C_1 R^2 \delta_{\alpha\beta} + C_2 R_\alpha R_\beta), \\ C_1 &= \frac{5 + 4s + 6\sigma_{\text{T}}}{9(1 + \sigma_{\text{T}})}, \\ C_2 &= \frac{(4s-1)(2\sigma_{\text{T}} - 1)}{9(1 + \sigma_{\text{T}})},\end{aligned}\quad (4.5)$$

where  $R$  is measured in the units of  $L$  and time  $t$  is measured in the units of  $\tau_L \equiv \tau(\ell = L)$ . The parameter  $\sigma_{\text{T}}$  is defined by analogy with Eq. (2.17):

$$\sigma_{\text{T}} \equiv \frac{\nabla \cdot \mathbf{D}_{\text{T}} \cdot \nabla}{\nabla \times \mathbf{D}_{\text{T}} \times \nabla} = \frac{\nabla_\alpha \nabla_\beta D_{\alpha\beta}^{\text{T}}(\mathbf{R})}{\nabla_\alpha \nabla_\beta D_{\alpha'\beta'}^{\text{T}}(\mathbf{R}) \epsilon_{\alpha\alpha'\gamma} \epsilon_{\beta\beta'\gamma}}, \quad (4.6)$$

where  $\epsilon_{\alpha\beta\gamma}$  is the fully antisymmetric unit tensor. Equations (2.17) and (4.6) imply that  $\sigma_{\text{T}} = \sigma_v$  in the case of  $\delta$ -correlated in time compressible velocity field.

For a random incompressible velocity field with a finite correlation time the tensor of turbulent diffusion  $D_{\alpha\beta}(\mathbf{R}) = \tau^{-1} \langle \xi_\alpha(\mathbf{r}_1|t) \xi_\beta(\mathbf{r}_2|t) \rangle$  (see [5]) and the degree of compressibility of this tensor is

$$\sigma_{\text{T}} = \frac{\langle (\nabla \cdot \boldsymbol{\xi})^2 \rangle}{\langle (\nabla \times \boldsymbol{\xi})^2 \rangle}. \quad (4.7)$$

To determine the functions  $B(\mathbf{R})$  and  $\mathbf{U}(\mathbf{R})$  we use the general form of the two-point correlation function of the droplets velocity field in the the range of scales  $\eta \leq \ell \ll \ell_*$ :

$$\begin{aligned}\langle v_\alpha(t, \mathbf{r}) v_\beta(t + \tau, \mathbf{r} + \mathbf{R}) \rangle &= \frac{1}{3} [\delta_{\alpha\beta} \\ &- R^{2(s-2)/3} (C_1^v R^2 \delta_{\alpha\beta} + C_2^v R_\alpha R_\beta)] f(\tau), \\ C_1^v &= \frac{(4 + s + 3\sigma_v)}{3(1 + \sigma_v)}, \\ C_2^v &= \frac{(1 + s)(2\sigma_v - 1)}{3(1 + \sigma_v)}.\end{aligned}\quad (4.8)$$

Substitution Eq. (4.8) into Eq. (4.3) yields

$$\begin{aligned}\mathbf{U}(\mathbf{R}) &= U_0 R^{(4s-7)/3}, \\ B(\mathbf{R}) &= B_0 R^{(4s-7)/3},\end{aligned}\quad (4.9)$$

where

$$U_0 = \beta \frac{\sigma_v}{\sigma_v + 1}, \quad B_0 = \alpha U_0$$

and the coefficients  $\alpha$  and  $\beta$  depend on the properties of turbulent velocity field. The dimensionless functions  $B_0$  and  $U_0$  in Eq. (4.9) are measured in the units of  $\tau_L^{-1}$ .

For the  $\delta$ -correlated in time random Gaussian compressible velocity field  $\sigma_{\text{T}} = \sigma_v$  and

$$B(\mathbf{R}) = \nabla_\alpha \nabla_\beta \hat{D}_{\alpha\beta}(\mathbf{R}), \quad (4.10)$$

$$U_\alpha(\mathbf{R}) = \nabla_\beta \hat{D}_{\alpha\beta}(\mathbf{R}) \quad (4.11)$$

(for details see [5, 12, 13]). In this case the second moment  $\Phi(t, \mathbf{R})$  can only decay, in spite of the compressibility of the velocity field.

For the finite correlation time of the turbulent velocity field  $\sigma_{\text{T}} \neq \sigma_v$  and Eqs. (4.10) and (4.11) are not valid. The clustering instability depends on the ratio  $\sigma_{\text{T}}/\sigma_v$ . In order to provide the correct asymptotic behaviour of Eq. (4.9) in the limiting case of the  $\delta$ -correlated in time

random Gaussian compressible velocity field we have to choose the coefficients  $\beta$  and  $\alpha$  in the form:

$$\beta = 8(4s^2 + 7s - 2)/27, \quad \alpha = (4s + 2)/3.$$

Note that when  $s < 1/4$  the parameters  $\beta < 0$  and  $B(\mathbf{R}) < 0$ . In this case there is no clustering instability of the second moment of droplets number density.

Thus, Eq. (4.1) in a non-dimensional form reads:

$$\frac{\partial \Phi}{\partial t} = R^{(4s-7)/3} [R^2 \Phi''(C_1 + C_2) + 2R \Phi'(U_0 + C_1) + B_0 \Phi]. \quad (4.12)$$

Consider a solution of Eq. (4.12) in the vicinity of the thresholds of the excitation of the clustering instability, where  $(\partial \Phi / \partial t) R^{(7-4s)/3}$  is very small. Thus, the solution of (4.12) in this region is

$$\Phi(R) = A_1 R^{-\lambda_1}, \quad (4.13)$$

where  $\lambda_1 = \lambda \pm i\mu$ ,

$$\lambda = \frac{C_1 - C_2 + 2U_0}{2(C_1 + C_2)}, \quad \mu = \frac{C_3}{2(C_1 + C_2)},$$

$$C_3^2 = 4B_0(C_1 + C_2) - (C_1 - C_2 + 2U_0)^2.$$

Since the correlation function  $\Phi(R)$  has a global maximum at  $R = a$ , the coefficient  $C_1 > C_2 - 2U_0$  if  $\mu$  is a real number (see below). Thus the asymptotic solution of the equation for the two-point correlation function  $\Phi(t, \mathbf{R})$  of the droplets number density in the range of scales  $a \leq \ell \leq \ell_*$  reads

$$\Phi(R) = A_1 R^{-\lambda} \sin[\mu \ln(\ell_*/R)], \quad (4.14)$$

where

$$A_1 = \left(\frac{L}{a}\right)^\lambda \frac{1}{\sin[\mu \ln(\ell_*/a)]}.$$

Now consider the range of scales  $\ell_* \ll \ell \ll L$ . In this case the nondimensional form of the turbulent diffusion tensor is given by

$$D_{\alpha\beta}^\top(\mathbf{R}) = R^{-2/3} (\tilde{C}_1 R^2 \delta_{\alpha\beta} + \tilde{C}_2 R_\alpha R_\beta), \quad (4.15)$$

$$\tilde{C}_1 = \frac{2(5 + 3\tilde{\sigma}_T)}{9(1 + \tilde{\sigma}_T)}, \quad \tilde{C}_2 = \frac{4(2\tilde{\sigma}_T - 1)}{9(1 + \tilde{\sigma}_T)},$$

and Eq. (4.1) reads:

$$\frac{\partial \Phi}{\partial t} = R^{-2/3} [R^2 \Phi''(\tilde{C}_1 + \tilde{C}_2) + 2R \Phi' \tilde{C}_1]. \quad (4.16)$$

Here we took into account that in this range of scales the functions  $B(\mathbf{R})$  and  $\mathbf{U}(\mathbf{R})$  are negligibly small, and the degree of compressibility of the turbulent diffusion tensor can be different in the above two ranges of scales.

Consider a solution of Eq. (4.16) in the vicinity of the thresholds of the excitation of the clustering instability, when  $(\partial \Phi / \partial t) R^{2/3}$  is very small. Thus, the solution of (4.16) is given by

$$\Phi(R) = A_2 R^{-\lambda_2}, \quad (4.17)$$

where

$$\lambda_2 = \frac{|\tilde{C}_1 - \tilde{C}_2|}{\tilde{C}_1 + \tilde{C}_2} = \frac{|7 - \tilde{\sigma}_T|}{3 + 5\tilde{\sigma}_T},$$

The growth rate of the second moment of droplets number density can be obtained by matching the correlation function  $\Phi(R)$  and its first derivative  $\Phi'(R)$  at the boundary of the above two ranges of scales, i.e., at the points  $R = \ell_*/L$ . The matching yields that in the range of scales  $\ell_* \ll \ell \leq L$  the asymptotic solution of the equation for the two-point correlation function  $\Phi(t, \mathbf{R})$  has the form of Eq. (4.17) with

$$A_2 = (-1)^k A_1 \left(\frac{\ell_*}{L}\right)^{\lambda_2 - \lambda + 1} \frac{\mu}{\lambda_2}.$$

Such matching is possible only when  $\lambda_1$  is a complex number, i.e., when  $C_3^2 > 0$  (i.e.,  $\mu$  is a real number). The latter determines the necessary condition for the clustering instability of droplets spatial distribution. The range of parameters  $(\sigma_v, \sigma_T)$  for which the clustering instability of the second moment of droplets number density may occur is shown in Fig. 1. The various curves indicate results for different value of the parameter  $s$  (see below). The line  $\sigma_v = \sigma_T$  corresponds to the  $\delta$ -correlated in time random compressible velocity field for which the clustering instability cannot be excited. The value  $s = 7/4$  corresponds to the turbulent diffusion tensor with the scaling  $\propto R^2$  [see Eq. (4.5)]. The curves for  $s = 7/4$  (dashed) and  $\kappa = 5/3$  (solid) practically coincide. The parameter  $s$  can be considered as a phenomenological parameter, and the change of this parameter from  $s = 5/3$  to  $s = 0$  can describe a transition from one asymptotic behaviour (in the range of scales  $a \leq \ell \leq \ell_*$ ) to the other ( $\ell_* \ll \ell \leq L$ ).

## V. DISCUSSION

### A. Parameters of turbulent spray in diesels

The diesel engines and the direct injection gasoline engines utilize liquid fuel sprays in order to increase the fuel surface area and thus to increase the vaporization and combustion rate. The liquid fuel injected into the combustion chamber breaks up into a large number of droplets of various sizes. During the ignition delay the droplets shatter and vaporize producing the fuel vapor, which is mixed with the surrounding ambient air. The combustion rate and the quality of combustion depend on the degree of the spray dispersion and on the amount of droplets to be vaporized during the time of ignition delay. In the direct injection engines excessive emission of pollutants and unburned hydrocarbons can result from poor injector performance. The degree of atomization required depends primarily upon the time available for the vaporization-mixing process. In a diesel engine, for example, this time is of the order of a few milliseconds

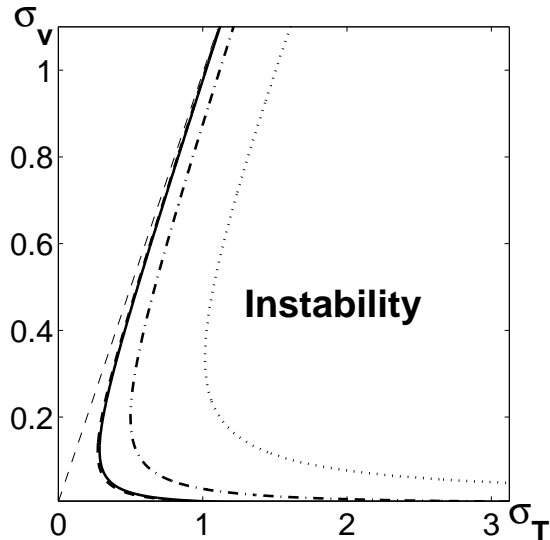


FIG. 1: The range of parameters  $(\sigma_v, \sigma_T)$  for which the clustering instability may occur. The various curves indicate the results for  $s = 7/4$  (dashed),  $\kappa = 5/3$  (solid), for  $s = 1$  (dashed-dotted) and for  $s = 2/3$  (dotted). The thin dashed line  $\sigma_v = \sigma_T$  corresponds to the  $\delta$ -correlated in time random compressible velocity field.

and thus very small droplets are required, see, e.g. Appendix A.

Since the rate of the droplets vaporization depends on the droplets sizes (proportional approximately to the droplets diameter), it strongly depends on the droplet size distribution. For the sprays consisting of droplets with a very small size (less than  $10 \mu\text{m}$ ) the droplets vaporize very quickly and the spray may be considered as a gas jet. Since the theory of droplet break up is still in an empirical state and it is not adequate to predict the size distribution of droplets in practical sprays, we will use the experimental data. For the numerical estimates we assume that the typical droplet size distribution for diesel conditions [3, 21] consists of majority of droplets of diameter  $40 \mu\text{m}$  with the minimum droplet sizes of  $10 \mu\text{m}$  and the maximum droplet size of  $100 \mu\text{m}$ . The small droplets are moving with almost zero velocity relative to the flow velocity of the air, but as it was shown in the previous sections, they are considerably influenced by the turbulent eddies which are typically  $(200 \div 300) \mu\text{m}$  in size as compared with  $(10 \div 100) \mu\text{m}$ -size droplets.

The role of the turbulent flow field in the combustion chamber is twofold. The intensity of turbulence should be high enough to provide a high quality fuel-air mixing. On the other hand, it was shown in the previous sections that in the turbulent flow field with sufficiently high intensity, the droplets spatial distribution becomes unstable with respect to formation of the clusters with the number density that is much higher than the average droplets number density. Such clusters can be viewed

as an effective mechanism for formation of the droplets of larger size. This propensity for the clusters formation may effectively change the droplets size distribution shifting it to the droplets with larger sizes, and, consequently, change the vaporization rate. Obviously, the cluster formation is an undesirable process, that impairs the vaporization-mixing process. This imposes a limitation on the maximum value of the turbulence intensity. The possibility of the cluster formation depends on the intensity of turbulence in the combustion chamber and we arrive to the problem of optimizing the turbulence level to attain the most effective vaporization-mixing process.

The starting point is the above theoretical model that describes the droplets clustering. For numerical estimates we adopt the operating parameters for a typical diesel engines, taking the crankshaft rotational speed  $N=3000 \text{ rev/min}$ , that corresponds to the average piston speed,  $\bar{v}_p = 10^3 \text{ cm/s}$ , and the turbulent velocity  $v' \simeq 5 \cdot 10^2 \text{ cm/s}$ . Taking into account that the spatial integral space (the characteristic scale of the largest turbulent eddies) for this conditions is  $L \simeq 0.3 \text{ cm}$  [3], we find for the Reynolds number:

$$\mathcal{Re} = \frac{v'L}{\nu} \simeq 10^4, \quad \text{with} \quad (5.1)$$

$$v' \simeq 5 \cdot 10^2 \text{ cm/sec.}, \quad L \simeq 0.3 \text{ cm}.$$

Here the kinematic viscosity of air is  $\nu \approx 0.015 \text{ cm}^2/\text{s}$ . To estimate  $\nu$  we used the following values for the air density  $\rho_{\text{air}} = 0.025 \text{ g/cm}^3$  (at 62 atm. and  $T=860 \text{ K}$ ), and for kinematic viscosity

$$\nu = \nu_0 R^{(3-\gamma)/2}, \quad (5.2)$$

where  $R = (\rho_{\text{air}}/\rho_{\text{air},0}) \approx 15$  is the compression ratio. Then the Kolmogorov micro-scale is  $\eta \approx L/\mathcal{Re}^{3/4} \sim 3 \mu\text{m}$ . A more accurate estimate is

$$\eta \approx \frac{L}{(\mathcal{Re}/\mathcal{Re}_{\text{cr}})^{3/4}}, \quad (5.3)$$

where  $\mathcal{Re}_{\text{cr}} > 1$  is the critical value of  $\mathcal{Re}$  at which the laminar flow becomes unstable. Taking  $\mathcal{Re}_{\text{cr}} \approx 5$ , we obtain a more realistic value  $\eta \approx 10 \mu\text{m}$ .

## B. Parameters of the clustering instability

### 1. Region of unstable cluster scales: $\eta < \ell < \ell_*$

Assuming the fuel density in droplets  $\rho_{\text{dr}} = 0.85 \text{ g/cm}^3$ , we find from the expression (3.18) the estimate for the critical value of the droplet radius,  $a_* \approx 4 \mu\text{m}$ , indicating that all droplets with  $a > 4 \mu\text{m}$  are unstable against formation of the clusters with scales ranging from  $\eta$  to  $\ell_*$ . This equation yields the following values of  $\ell_*$ :  $\ell_* \approx 160 \mu\text{m}$  for  $a = 10 \mu\text{m}$  and  $\ell_* \approx 1 \text{ cm}$  for  $a = 40 \mu\text{m}$ .

### 2. Characteristic times of clustering, $\tau_{cl}$

The characteristic time of the cluster growth  $\tau_{cl}(\ell) = 1/\gamma_{cl}$  depends on the cluster size  $\ell$ . Estimate for  $\ell = \ell_*/3$  gives  $\tau_{cl}(\ell_*/3) \approx 1.7\tau(\ell_*) \approx \tau_{dr}$ . The turnover time  $\tau(\ell)$  can be estimated as follows:

$$\tau(\ell) \simeq 5 \left(\frac{L}{v'}\right) \left(\frac{\ell}{L}\right)^{2/3} \simeq 3 \times 10^{-3} \left(\frac{\ell}{L}\right)^{2/3} \text{ sec} . \quad (5.4)$$

Here we used our estimates (5.1) for the integral scale  $L$  and turbulent velocity  $v'$ . Assuming for the droplets with the size  $a = 10 \mu\text{m}$ ,  $\ell = \ell_*/3 \approx 50 \mu\text{m}$  (with  $\ell_* = 160 \mu\text{m}$ ) one has  $\tau_{cl}(\ell) \approx 0.35 \mu\text{s}$ . For the droplets with the radius  $a = 40 \mu\text{m}$  with  $\ell_* \approx 1 \text{ cm}$ , one has  $\tau_{cl}(\ell_*/3) \approx 5.5 \mu\text{s}$ , which is larger than the characteristic spray time in the combustion chamber (a few milliseconds). These estimates imply that for the chosen parameters the distribution of the droplets in the spray will be shifted to the droplets with larger diameters at the given turbulent intensity.

### 3. Time of the turbulent air-fuel mixing, $\tau_T$

Now we estimate the time of the turbulent air-fuel mixing,  $\tau_T \simeq 1/\gamma_T$  in the combustion chamber. Taking into account that

$$\gamma_T = \frac{D_T}{d^2} = \frac{v'L}{3d^2}, \quad (5.5)$$

where  $D_T$  is the coefficient of turbulent diffusion, and  $d \simeq 10 \text{ cm}$  is the bore diameter, we find for the time of turbulent air-fuel mixing  $\tau_T \approx 1 \text{ s}$ . Thus, the turbulent diffusion itself is too slow and a strong external global flow - "swirl" is needed for the effective air-fuel mixing.

### C. Droplets number density in saturated clusters

In the previous sections we have shown that the droplets spatial distribution in the turbulent flow field is unstable against formation of clusters with droplets number density that is much higher than the average droplets number density. Obviously this exponential growth at the linear stage of instability should be saturated by nonlinear effects. The nonlinear saturation for the water droplets in the atmospheric turbulence (in clouds) was discussed in Ref. [5]. Here we discuss a similar issue for the fuel droplets under the typical conditions pertinent to diesel engines.

A momentum coupling of particles and turbulent fluid is essential when  $m_{dr}n_{cl} \sim \rho_{air}$ , i.e., the mass loading parameter,  $\phi = m_{dr}n_{cl}/\rho_{air}$ , is of the order of unity (see, e.g., [22]). This condition implies that the kinetic energy of air  $\rho_{air}\langle \mathbf{u}^2 \rangle$  is of the order of the droplets kinetic energy  $m_{dr}n_{cl}\langle \mathbf{v}^2 \rangle$ , where  $|\mathbf{u}| \sim |\mathbf{v}|$ . This yields:

$$n_{cl} \sim a^{-3}(\rho_{air}/3\rho_{dr}) . \quad (5.6)$$

For the fuel droplets in the diesel combustion chambers (see, e.g. [1] and Appendix A)  $\rho_{dr}/\rho_{air} \simeq 34$ . Thus, e.g., for  $a \simeq 10 \mu\text{m}$  we obtain  $n_{cl} \sim 3 \times 10^7 \text{ cm}^{-3}$ . For the cluster with the size  $\ell \approx \ell_*/3 \approx 50 \mu\text{m}$  this yields for the total number of particles in the cluster of that size  $N_{cl} \simeq \ell^3 n_{cl} \sim 30$ . This values may be considered as a lower estimate for the "two-way coupling" when the hydrodynamic effect of the air on droplets has to be considered together with the feed-back effect of the droplets on the carrier air.

Note that according to Ref. [22], the turbulence modification by droplets is governed by the ratio of the droplet energy and the total energy of the suspension (rather than the energy of the carrier air) and thus by parameter  $\phi(1+\phi)$  (rather than by  $\phi$  itself). Thus we expect that the two-way coupling can only mitigate but not to prevent from the excitation of the clustering instability. An actual mechanism of the nonlinear saturation of the clustering instability is a "four way coupling" in which the droplet-droplet interaction is also important. In this situation the droplet collisions result in the effective droplet pressure which prevents further grows of concentration.

Droplets collisions play essential role when the total number of collisions is of the order of the number of droplets in the cluster during the life-time of a cluster. The rate of collisions  $J \sim n_{cl}/\tau_{coll}$  can be estimated as  $J \sim 4\pi a^2 n_{cl}^2 v_{rel}$ . The relative velocity  $v_{rel}$  of colliding particles with different but comparable sizes can be estimated as  $v_{rel} \sim \tau_{dr} |(\mathbf{u} \cdot \nabla)\mathbf{u}| \sim \tau_{dr} u_\ell^2/\ell$ , where  $\ell$  is the cluster size. Thus the collisions in clusters may be essential for

$$n_{cl} \sim \frac{\ell}{a^4} \frac{\rho_{air}}{3\rho_{dr}}, \quad (5.7)$$

that is larger than the estimate given by Eq. (5.6) by a factor  $\ell/a$ . In the above example ( $a \simeq 10 \mu\text{m}$ ,  $\ell \approx 50 \mu\text{m}$ ) this gives  $n_{cl} \sim \times 10^8 \text{ cm}^{-3}$  and  $N_{cl} \sim 150$ . For larger droplets with radius  $a \simeq 40 \mu\text{m}$  we estimated  $\ell = \ell_*/3 \approx 0.3 \text{ cm}$ . In this case  $n_{cl} \sim 3 \times 10^7 \text{ cm}^{-3}$  with the total number of particles in the cluster  $N_{cl} \sim 10^6$ . Note that the mean number density of droplets in a combustion camera  $\bar{n}$  is about  $10^4 \text{ cm}^{-3}$ . Therefore the clustering instability of droplets in the internal combustion engines increases their concentrations in the clusters by the orders of magnitude.

### Acknowledgments

This research was supported in part by The German-Israeli Project Cooperation (DIP) administrated by the Federal Ministry of Education and Research (BMBF), by Swedish Ministry of Industry (Energimyndigheten, contract P 12503-1), by the Swedish Royal Academy of Sciences, the STINT Fellowship program, by the Israel Science Foundation governed by the Israeli Academy of Science and by INTAS Program Foundation (Grant No. 00-0309).

**APPENDIX A: INFO FOR PEDESTRIANS:  
TYPICAL PARAMETERS FOR DIRECT  
INJECTION AND DIESEL ENGINES, [1]**

- *Cylinder.* Diameter 7÷12 cm, height: 8÷13 cm. Speed rate:  $S=3600\div 5000$  rev/min =60÷85 rev/sec. The cylinder pressure: 50÷100 atm. Air in the combustion chamber is heated by the adiabatical compression up to 1000÷1200 K. Typical compression ratio  $R = [\rho_{\text{air}}/\rho_{\text{air},0}] \approx 15 \div 20$ .

- *Fuel injection geometry.* Nozzle diameter: 0.15÷0.35 mm. The spray cone angle: between 5 and 15 degrees and is affected more by the fluid viscosity and surface tension than by the hole diameter  $d$ , or  $d/L$ . Using the plain orifice with the swirl atomizer increases the spray angle up to 90 degrees.

- *Fuel injection.* Injection pressure 300÷1500 atm.

The initial fuel jet speed 200÷300 m/s. Swirl velocity: 8÷20 m/s. Injection time,  $T_{\text{inj}} \approx T/16$ , where  $T$  is the period. Hence,  $T_{\text{inj}} = (0.7 \div 1) \times 10^{-3}$  s, and time available for the vaporization can be as short as a few milliseconds.

- *Turbulence in the combustion cameras.* Turbulent eddies size (longitudinal integral scale of turbulence) are typically 0.2÷0.5 cm in size, decreasing with the compression ratio. The average turbulence intensity (mean root square of longitudinal velocity fluctuation) varies almost linearly to the mean piston speed with a constant 0.5÷0.6.

- *Fuel spray properties.* Fuel density  $\rho_{\text{dr}} = 0.85$  g/cm<sup>3</sup>. Fuel droplet diameter about 10÷100 μm. Air density  $\rho_{\text{air}} = 0.025$  g/cm<sup>-3</sup> (at 62 atm. and  $T = 860$ K). For these values  $\rho_{\text{dr}}/\rho_{\text{air}} = 34$ . Kinematic viscosity  $\nu = \nu_0 R^{(3-\gamma)/2}$ . For  $R = 15$ ,  $\nu \approx 0.015$  cm<sup>2</sup> /s.

- 
- [1] J.B. Heywood, *Internal Combustion Engine Fundamentals*, (MacGraw-Hill, Boston-New-York, 1988).
- [2] T. Kamimoto and H. Kobayashi, *Prog. Energy Combust. Sci.* **17**, 163 (1991).
- [3] G.L. Borman and K.W. Ragland, *Combustion Engineering*, (MacGraw-Hill, Boston-New-York, 1999).
- [4] J. Bellan, *Progress in Energy and Combust. Sci.* **28**, 329 (2000).
- [5] T. Elperin, N. Kleeorin, V. L'vov, I. Rogachevskii and D. Sokoloff, *Phys. Rev. E* **66**, 036302 (2002). Also: nlin.CD/0202048 and nlin.CD/0204022.
- [6] T. Elperin, N. Kleeorin and I. Rogachevskii, *Phys. Rev. Lett.* **77**, 5373 (1996).
- [7] C.T. Crowe, M. Sommerfeld and Y. Tsuji, *Multiphase Flows with Particles and Droplets* (CRC Press, NY, 1998).
- [8] R.A. Shaw, *Ann. Rev. Fluid Mech.* **35**, 183 (2003).
- [9] J.R. Fessler, J.D. Kulick and J.K. Eaton, *Phys. Fluids* **6**, 3742 (1994).
- [10] A. Aliseda, A. Cartellier, F. Hainaux and J.C. Lasheras, *J. Fluid Mech.* **468**, 77 (2002).
- [11] T. Elperin, N. Kleeorin and I. Rogachevskii, *Phys. Rev. Lett.* **76**, 224 (1996); **80**, 69 (1998); **81**, 2898 (1998).
- [12] T. Elperin, N. Kleeorin, I. Rogachevskii and D. Sokoloff, *Phys. Chem. Earth*, **A 25**, 797 (2000).
- [13] T. Elperin, N. Kleeorin, I. Rogachevskii and D. Sokoloff, *Phys. Rev. E* **63**, 046305 (2001).
- [14] R.H. Kraichnan, *Phys. Fluids* **11**, 945 (1968).
- [15] L.D. Landau and E.M. Lifshits, *Fluid mechanics* (Pergamon, Oxford, 1987).
- [16] A.S. Monin and A.M. Yaglom, *Statistical Fluid Mechanics: Mechanics of Turbulence* (M.I.T. Press, Cambridge, 1975), vol. 2.
- [17] U. Frisch, *Turbulence: The Legacy of A. N. Kolmogorov* (Cambridge University Press, Cambridge 1995).
- [18] J.L. Lumley, in *Two-Phase and Non-Newtonian Flows, Turbulence*, ed. P. Bradshaw, (Springer Verlag, Berlin, 1976).
- [19] V.S. L'vov and I. Procaccia, in *Lecture Notes of the Les Houches Summer School "Fluctuating Geometries in Statistical Mechanics and Field Theory"*, ed. by F. David and P. Ginsparg, (North-Holland, Amsterdam, 1995).
- [20] V.S. L'vov and I. Procaccia, *Phys. Rev. E* **52**, 3840 (1995); **52**, 3858 (1995).
- [21] H.H. Chiu, *Prog. Energy and Combust. Sci.* **26**, 381 (2000).
- [22] V.S. L'vov, G. Ooms and A. Pomyalov, *Phys. Rev. E* **67**, 046314 (2003). Also: nlin.CD/0210069.